Conf-901194--16

To be presented at the 1990 American Society of Mechanical Engineers (ASME) Winter Annual Meeting (WAM) in Dallas, TX in November 25-30, 1990.

BNL--44530

DE91 010373

COIL AND IRON DESIGN FOR SSC 50 MM MAGNET†

R.C. Gupta, S.A. Kahn and G.H. Morgan
Accelerator Development Department
Brookhaven National Laboratory
Upton, NY 11973 USA

APR 15 1991

Abstract

In this paper we present the design of the two dimensional coil and iron cross section, referred[1] to as DSX201/W6733, for the 50 mm aperture dipole magnet being built at the Brookhaven National Laboratory for the Superconducting Super Collider (SSC). The computed values of the allowed field harmonics as a function of current, the quench performance predictions, the stored energy calculations, the effect of random errors on the coil placement and the Lorentz forces on the coil will be presented. The yoke has been optimized to reduce iron saturation effects on the field harmonics. We shall present the summary of this design which will include the expected overall performance of this cross section.

Introduction

It has been decided to increase the aperture of the superconducting dipole magnet from 40 mm to 50 mm. In addition, it was recommended by the SSC 5 cm Dipole Task Force[2] to use wider cables than those used in the 4 cm dipole[3] to obtain a field margin of 10% over 6.6 tesla. From beam dynamics considerations, this dipole is required to have smaller values of field harmonics and a lower variation in them due to iron saturation than those originally specified for the SSC 4 cm dipole magnet.

The coil aperture in this magnet will actually be 49.56 mm instead of 50 mm. This reflects a slight change in the width of the cable used in the inner layer. Moreover, the thickness of the cable used in the outer layer was also changed. These modifications produce a small change in the values of field harmonics from their design value. An iteration in the basic coil design brings the harmonics back close to their original values. However, due to various reasons the harmonics in the manufactured coil usually come out to be somewhat different than what the coil was designed for. Therefore, to avoid delay in the magnet program, an iteration to obtain the desired harmonics in the production magnet could be incorporated after a few magnets are made.

Coil Design

The coil is made of two layers of superconducting cables. Some basic parameters of the cables used in the inner and outer layers are shown in Table 1. The cable used in the inner layer has 30 strands and in the outer layer 36.

The coil is designed by placing the cables in such a way that they produce a field to a high degree of uniformity. This is done using the computer program PAR2DOPT[4] which uses analytic expressions for computing the field harmonics at the center of the magnet of coils in a circular iron aperture. It also computes the peak field on the surface of the conductor.

We examined numerous configurations for the coil design. The one selected has a total number of 45 turns in each quadrant in two layers. The inner layer has 19 turns in four blocks (three wedges) and the outer has 26 turns in two blocks (one wedge). During the coil optimization process, we closely monitored the peak field, i.e., the maximum value of magnetic field in the conductor, both in the inner and in the outer layer. For the same transfer function, a coil design with a lower peak field would produce a magnet which will quench at a higher current. In our search for the most optimum coil configuration, we kept the number of wedges in the outer layer to be one; however in the inner we looked for solutions with two or three wedges. The designs with two wedges in the inner layer were, in general, found to have a higher peak field or excessive harmonic content. For this reason, we chose a design having three wedges in the inner layer. The SSC 4 cm magnet also has three wedges in the inner layer and one in the outer. However, the present coil is optimized in such a way that the two wedges nearest to the pole in the inner layer are identical and symmetric. This design has performance comparable to those which did not have this imposition on the two wedges.

The physical layout of the optimized coil configuration is shown in Fig. 1.

†This work has been suuported by U.S. Department of Energy.

MASTER

DISTRIBUTION OF THIS DOCUMENT IS UNLIMITED

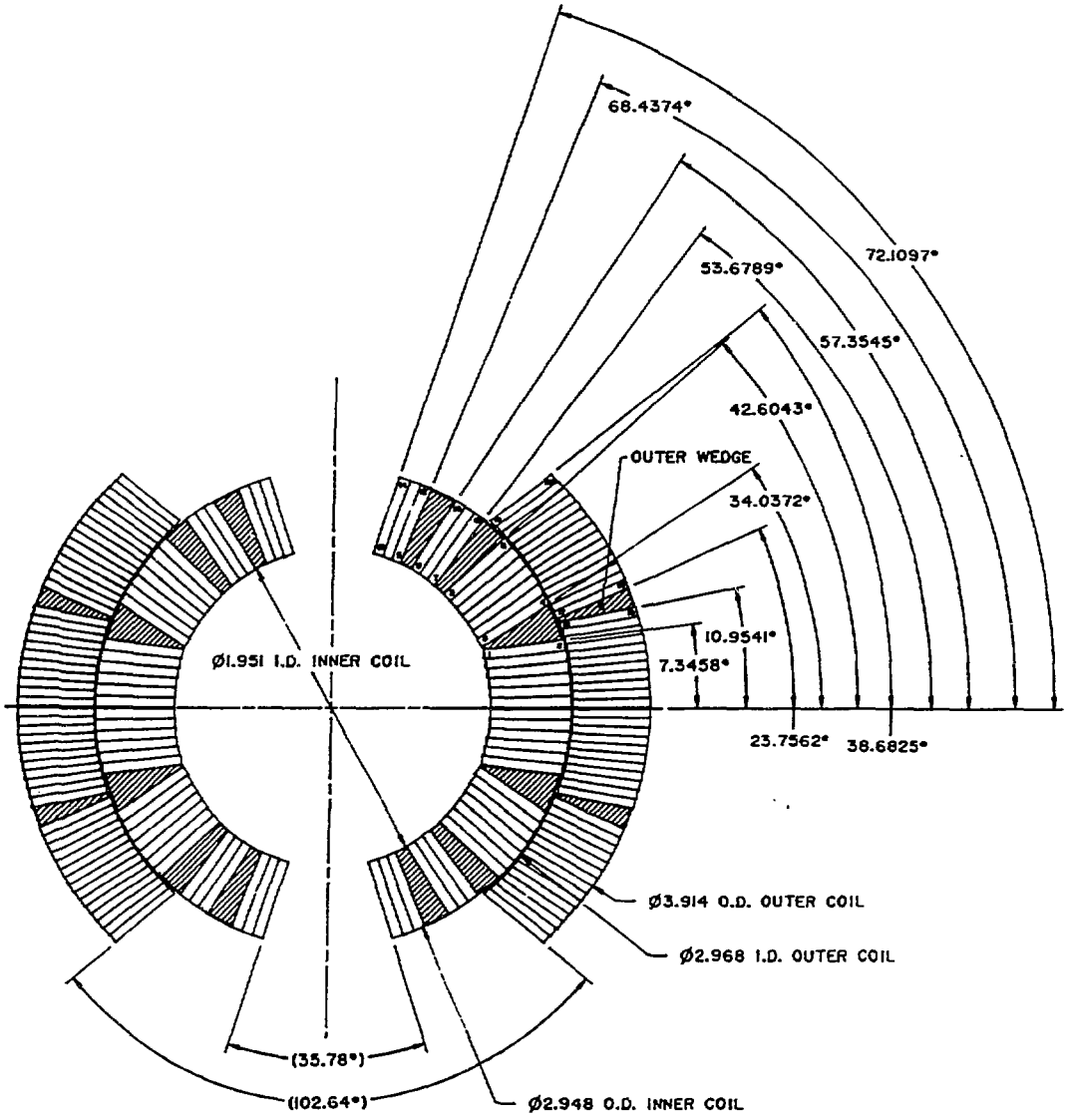

Figure 1: Optimized Coil for SSC 50 mm Dipole.

Table 1: Cable properties of SSC 50 mm magnet with wider cables.

Cable parameters	Inner layer	Outer Layer
Filament diameter, micron	6.0	6.0
Strand diameter, mm	0.808	0.648
No. of strands	30	36
No. of strands × Strand Area, mm^2 (Approximate cable area)	15.382	11.872
Cable width, bare, mm	12.34	11.68
Cable width, insulated, mm	12.51	11.85
Cable mid-thickness, bare, mm	1.458	1.156
Cable mid-thickness, insulated, mm	1.626	1.331
Keystone, (max-min) thickness, mm	0.262	0.206

Table 2: Desired and Optimized values of *low field* harmonics in prime units. The harmonics *in magnet* take into account the pole notch and a flat face in the iron at the midplane. These harmonics are in the units of 10^{-4}

Values	b_2'	b_4'	b_6'	b_8'	b_{10}'	b_{12}'
Desired	-.28±.4	.01±.1	0±.05	±(.04to.05)	0±.05	0±.05
Optimized	-0.280	0.009	-0.004	0.044	0.014	-0.001
In magnet	0.000	-0.001	-0.004	0.044	0.014	-0.001
Revised	1.566	0.070	-0.024	0.043	0.015	-0.001

Low Field Harmonics

The iron aperture is not completely circular in this magnet. It has a pole notch and a small vertical straight face at the midplane. These structures introduce small but noticeable non-zero values of b_2' and b_4' harmonics. These harmonics should be cancelled out in a coil design if the magnet is to produce zero low field harmonics. Therefore, to cancel the effect of non-circular iron inner radius, -0.28 prime units of b_2' and +0.01 of b_4', were desired in the optimized coil. In addition, a non-zero value of b_8' harmonic was desired for centering the coil during the field measurements. Since the given tolerance in b_8' was 0.05 prime unit, we looked for a solution which had a magnitude of this harmonic between 0.04 and 0.05. This requirement on b_8' threw many designs out of running. However, the final design which satisfied all of above requirements was no worse in performance to those which did not.

In Table 2 we have given the desired and optimized values of field harmonics in prime units. Harmonics, higher than b_{12}', had an optimized value of < 0.001, as desired. In the row of desired harmonics, we have also listed the tolerances in them. *"In magnet"* harmonics takes into account the pole notch and a flat face in the iron at the midplane. These would be the expected values of low field harmonics in this magnet (However, it does not including the contributions from persistent currents in the superconductor). As mentioned earlier, for mechanical reasons, the size of the cable was changed by a small amount from the one assumed in the original design. This produces a small deviation in the field harmonics. The last row of the table, "Revised", refer to the values of field harmonics in the magnet after this change in the cable size.

We have used the following definition for field harmonics

$$B_y + iB_x = B_0 \sum_{n=0}^{\infty} [b_n + ia_n][cos(n\theta) + i\ sin(n\theta)] \left(\frac{r}{R_0}\right)^n,$$

where B_0 is the field at the center of the magnet, B_x and B_y the components of field at (r,θ), R_0 the normalization radius, a_n the skew harmonics and b_n the normal. These harmonics are usually quoted in prime units (b_n' and a_n') when R_0 is chosen to be 1 cm and the harmonics are given in 10^{-4} units.

Iron Yoke Design

In this section we shall discuss the process used in designing the iron yoke. The iron contributes about 22% to the magnetic field at 6.6 tesla (somewhat higher at lower field). Since the magnetization of the iron is not a linear function of current in the coil and since the magnetization of the iron is not the same throughout the cross section, the uniformity of the field becomes a function of the current in the coil. The yoke is optimized to produce a minimum change in field harmonics (due to iron saturation) for the maximum achievable value of transfer function at 6.6 tesla. We used computer codes POISSON, MDP and PE2D for this purpose. We shall compare the results of field computations done using these three codes. We shall discuss, in detail, the computer model of the final design and the results of field calculations for it with POISSON. An iron packing factor of 97.5% has been used in these calculations.

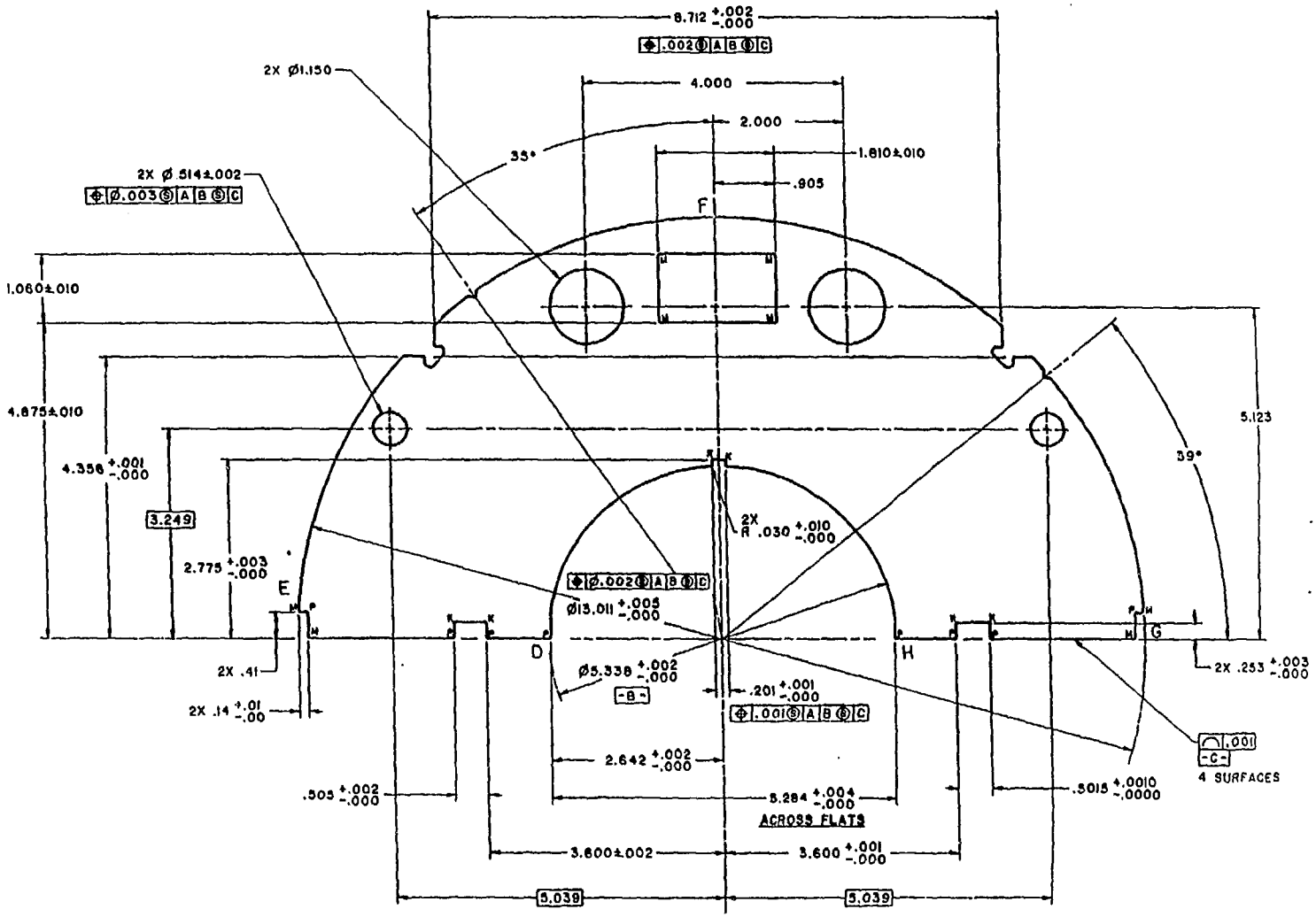

Figure 2: Optimized Yoke for SSC 50 mm Dipole.

Table 3: Transfer function and b_2' variation as function of current. In all cases b_2' is corrected to start from zero at 3.0 kA.

I	T.F. (T/kA)			$b_2' \times 10^{-4}$		
kA	POISSON	MDP	PE2D	POISSON	MDP	PE2D
3.0	1.0447	1.0430	1.0430	0.00	0.00	0.00
4.0	1.0441	1.0413	1.0423	0.09	0.05	0.12
5.0	1.0397	1.0364	1.0374	0.24	0.16	0.24
5.5	1.0340	1.0311	1.0319	0.27	0.21	0.36
6.0	1.0262	1.0236	1.0243	0.15	0.17	0.30
6.25	1.0219	1.0194	1.0201	0.08	0.11	0.19
6.5	1.0173	1.0148	1.0156	-0.02	0.03	0.21

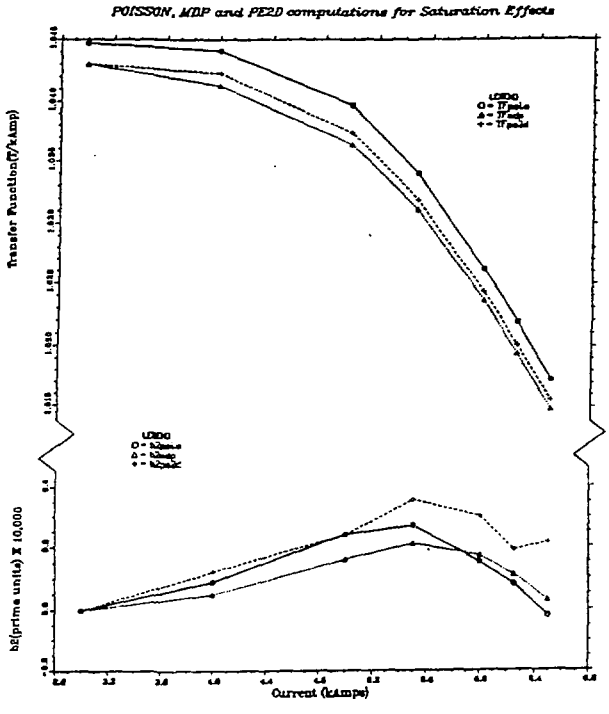

Figure 3: Transfer Function and b_2' as a function of current in SSC 50 mm Dipole, as computed by POISSON, MDP and PE2D.

If no special technique for controlling iron saturation were used, the change in b_2' harmonic due to iron saturation will be over 1 unit. This is more than the desired change of less than 0.6 unit. The following three options were considered for reducing the b_2' saturation swing. They all try to control the iron saturation at the iron aperture so that it saturates evenly.

- Reduced (shaved) iron o.d.
- Stainless Steel (non-magnetic) key at the midplane
- Shim at the iron inner surface

The first scheme, though most straight forward, produces the maximum loss in transfer function at 6.6 tesla as compared to the other two schemes. The third scheme, though actually increasing the transfer function at 6.6 tesla due to extra iron, requires more considerations from various point of view due to its non-circular aperture. The second scheme produces very little loss in transfer function (0.3% at 6.6 tesla compared to a keyless or magnetic key version) for a comparatively large reduction in b_2' saturation ($\frac{3}{4}$ unit). Moreover, it also has the advantage of giving a lever (within limits) for controlling b_2' saturation by changing the location and/or size of the key without affecting the other parts of the magnet design. This is so because nothing changes at the iron inner or outer surface. If the measurements don't match with the calculations due to any reason, then this could be a very useful and convenient handle to empirically correct the b_2 v/s I curve. In past, measurements and calculations have agreed to a few tenth of prime unit when the change in b_2' harmonic due to iron saturation was compared. It may be pointed out that besides iron saturation, b_2 and other harmonics are also a function of current because of the coil deformation due to Lorentz forces.

The optimized yoke is shown in Fig. 2. The iron i.d. is $5.339''$. This leaves a space of 17 mm for the collar. The iron o.d. is $13.0''$. This value is a slight reduction from the value ($13.22''$) obtained by extrapolation of the present 4 cm aperture design, and hence includes a bit of iron shaving. The stainless steel key is located at $3.6''$ and has a size of $\frac{1}{2}'' \times \frac{1}{2}''$. As mentioned earlier, the iron aperture is not completely circular. It has a pole notch of size $0.201'' \times 0.105''$ and a vertical straight face at the midplane which starts at $x = 2.643''$. Other structures in the yoke are shown in Fig. 2.

In Fig. 3 we plot transfer function (T.F.) and b_2' as a function of current as computed by POISSON, MDP and PE2D. The low field b_2' harmonic has been corrected so that it starts from zero; a non-zero value is artificial and is related to the way the computer model of a given coil and iron geometry is set up in these three codes. The values of the variables plotted in Fig. 3 is given in Table 3. The maximum b_2' saturation, as computed by the three codes is about 0.3 prime unit. The POISSON uses a generalized finite difference method, the MDP uses an integral method and PE2D uses the finite element method. Despite the fact that these three programs uses three different methods for solving the problem, it is encouraging to see that all predict a small saturation shift.

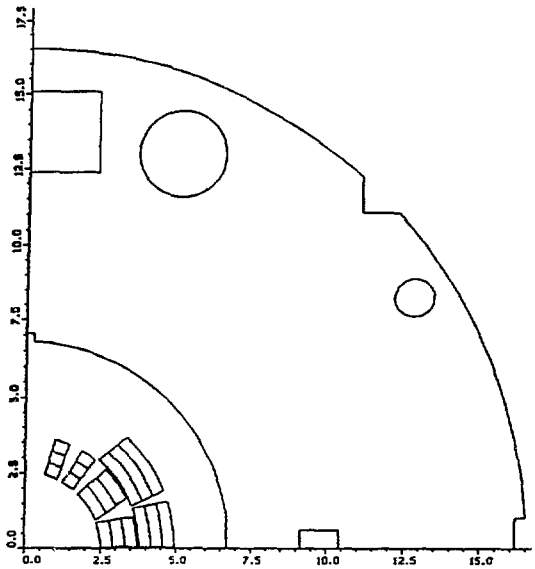

Figure 4: POISSON model for SSC 50 mm Dipole.

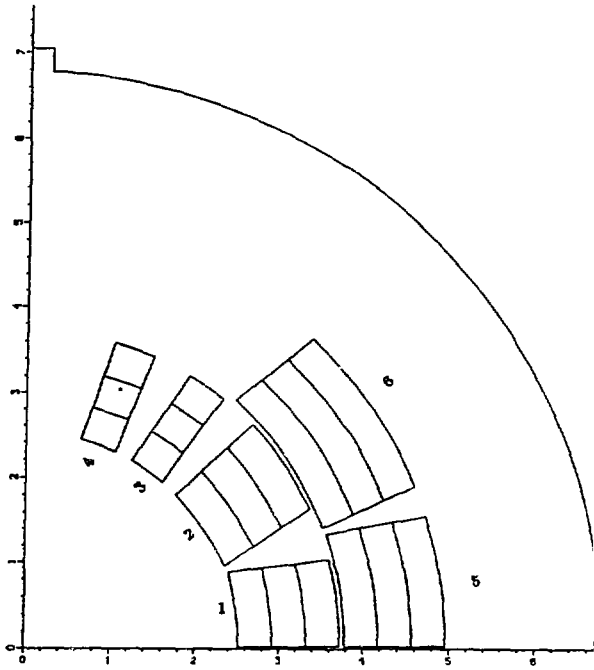

Figure 5: POISSON model of optimized Coil for SSC 50 mm Dipole.

In Table 4 we have listed the maximum change in b_2' and b_4' harmonics due to iron saturation. All other higher harmonics remain practically unchanged. In the same table we have also listed the drop in transfer function, $\delta(TF)$, till 6.6 tesla as compared to its value at low field.

Now we discuss the details of the computer model for the final design and the magnetic analysis for it using the computer code POISSON. It solves for the vector potential using a finite difference equation method with successive point over-relaxation. The POISSON model of SSC 50 mm Dipole is shown in Fig. 4. Each conductor block is divided in three radial sub-divisions to simulate a more realistic current distribution inside the cable. The conductor is shown in more detail in Fig. 5.

Table 4: Drop in transfer function till 6.6 tesla and the maximum change in b_2' and b_4'; higher harmonics remain practically unchanged.

Harmonic	POISSON	MDP	PE2D
$\delta(TF)$, till 6.6T	2.62%	2.70%	2.63 %
$\delta(b_2')_{max}$, 10^{-4}	0.28	0.22	0.36
$\delta(b_4')_{max}$, 10^{-4}	-0.03	-0.02	-0.04

In Table 5 we present the results of field calculations for various values of current per turn. In Fig. 6, we plot the variation of field harmonics as a function of central field.

Expected Quench Performance

The central field at which the cable looses its superconducting properties (B_{ss}, with "ss" standing for Short Sample) depends on the maximum magnetic field in the conductor (peak field), the bath temperature, the current density in the cable and the quality of the cable itself (degradation). We have listed the peak field (B_{pk}) in the inner and outer layers in Table 6 for two values of central field (B_o). The ratio of B_{pk} to B_o, the *Enhancement Factor*, is given in the next column. In each layer, the peak field is found on the upper edge of the top (pole) most turn. The location of it is expressed in % of the cable width as measured from the upper-left corner of that turn. In the next column we list this location. We have done the peak field calculations using the code MDP which is considered to be better suited to this purpose.

Our calculations assume that the superconducting wire will have a critical current density $J_c(5T, 4.2K)$ of 2750 amp/mm^2. The quality of the superconductor gets degraded when the cable is made out of these wires and put in the magnet. We have done calculations with 5% degradation (J_c=2612.5) in Table 7 at 4.35° kelvin bath temperature and in Table 8 at 4.0° kelvin.

Table 5: Results of POISSON computations for SSC 50 mm Dipole.

I kA	B_o tesla	T.F. T/kA	b_2' 10^{-4}	b_4' 10^{-4}	b_6' 10^{-4}	b_8' 10^{-4}	b_{10}' 10^{-4}	b_{12}' 10^{-4}
$\infty\mu$	$\infty\mu$	1.04493	0.020	-0.046	0.000	0.047	0.015	-0.001
3.000	3.1341	1.04471	0.031	-0.046	0.001	0.047	0.015	-0.001
4.000	4.1762	1.04406	0.111	-0.050	0.001	0.047	0.015	-0.001
4.500	4.6921	1.04268	0.140	-0.055	0.001	0.047	0.015	-0.001
4.750	4.9464	1.04135	0.182	-0.060	0.001	0.047	0.015	-0.001
5.000	5.1985	1.03969	0.255	-0.063	0.001	0.047	0.015	-0.001
5.250	5.4454	1.03721	0.299	-0.066	0.001	0.047	0.015	-0.001
5.500	5.6871	1.03402	0.291	-0.069	0.001	0.048	0.015	-0.001
5.750	5.9240	1.03027	0.235	-0.071	0.001	0.048	0.015	-0.001
6.000	6.1573	1.02621	0.172	-0.073	0.000	0.048	0.015	-0.001
6.250	6.3868	1.02189	0.100	-0.073	0.000	0.048	0.015	-0.001
6.500	6.6121	1.01725	-0.003	-0.072	0.000	0.048	0.015	-0.001
7.000	7.0513	1.00733	-0.300	-0.072	0.000	0.049	0.015	-0.001

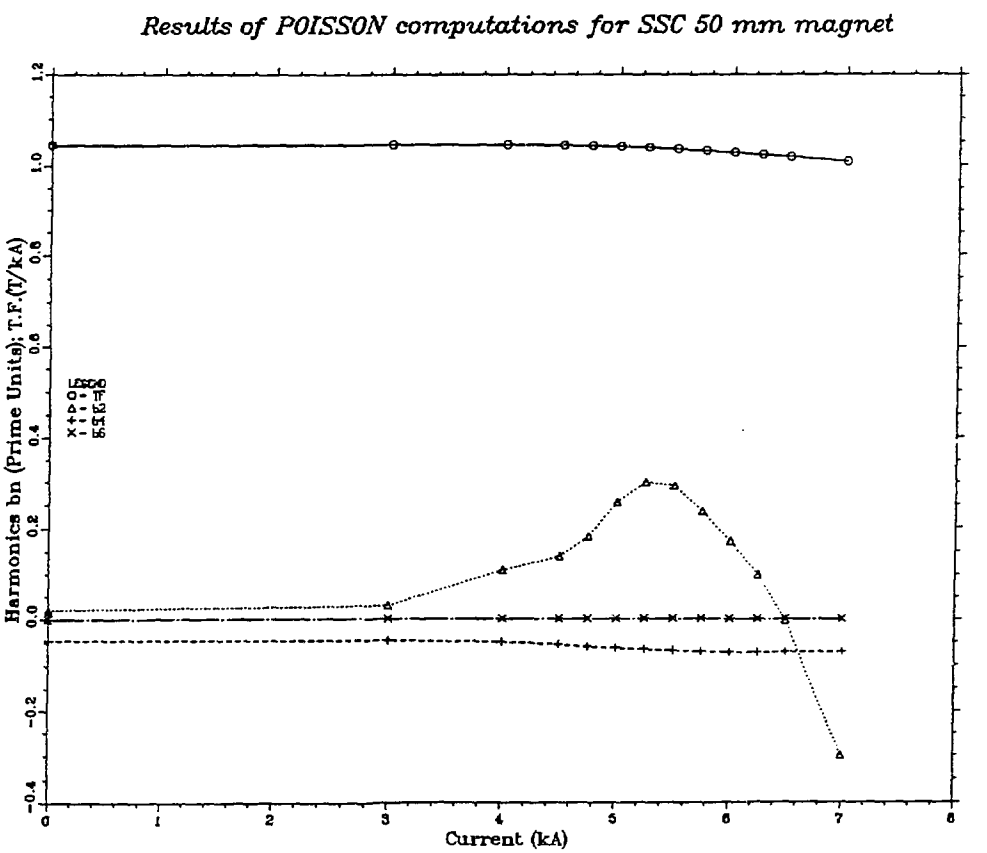

Figure 6: Variation in Field Harmonics as a function of B_o for SSC 50 mm magnet as computed by POISSON.

Table 6: Peak fields in SSC 50 mm Dipole as computed with MDP

I	B_o	Inner			Outer		
kA	tesla	B_{pk},T	$\frac{B_{pk}}{B_o}$	Location	B_{pk},T	$\frac{B_{pk}}{B_o}$	Location
6.85	6.9058	7.2374	1.048	5%	6.0016	0.869	11%
7.20	7.2100	7.5595	1.048	5%	6.2660	0.869	11%

Table 7: Expected quench performance of SSC 50 mm Dipole with 5% cable degradation ($J_c = 2612.5 amp/mm^2$) and at 4.35° kelvin bath temperature.

Layer ↓	Cu/Sc Ratio	B_{ss} tesla	I_c amp	B_{margin} %	T_{margin} kelvin	S_{quench} amp/cm^2	$S_{6.6T}$ amp/cm^2
Inner	1.7	7.149	7126	8.3	0.519	736	671
	1.5	7.273	7273	10.2	0.625	788	704
	1.3	7.399	7411	12.1	0.730	853	748
Outer	2.0	7.268	7267	10.1	0.580	919	822
	1.8	7.445	7470	12.8	0.709	980	852

Table 8: Expected quench performance of SSC 50 mm Dipole with 5% cable degradation ($J_c = 2612.5 amp/mm^2$) and at 4.0° kelvin bath temperature.

Layer ↓	Cu/Sc Ratio	B_{ss} tesla	I_c amp	B_{margin} %	T_{margin} kelvin	S_{quench} amp/cm^2	$S_{6.6T}$ amp/cm^2
Inner	1.7	7.455	7481	13.0	0.869	773	671
	1.5	7.571	7615	14.7	0.975	826	704
	1.3	~ 7.654	~ 7711	~16.0	~1.080	~ 888	~748
Outer	2.0	7.642	7697	15.8	0.930	973	822
	1.8	7.825	7908	18.6	1.059	1037	852

In these tables we have listed the Field Margin (B_{margin}) and the Temperature Margin (T_{margin}). The temperature margin is defined as the maximum possible computed rise in the operating temperature (over the design value of normal operation, which is 4.35° K) before which the magnet will quench at the design central field (B_{design}=6.5 tesla). The Field Margin is defined as follows

$$B_{margin}\,(\%) = \frac{B_{ss} - B_{design}}{B_{design}} \times 100$$

These calculations are less accurate when the peak field in the conductor, used in the $J_c(B,T)$ correlation, is greater than 8 tesla beyond which experimental data are not available. We have indicated these cases by putting ~ before the value of B_{ss}. In the outer layer a copper to superconductor ratio, CSR or Cu/Sc, of 2.0 and 1.8 is used in the calculations. In the inner layer we have done these calculations for Cu/Sc ratio being 1.7, 1.5 and 1.3. We have listed the computed central field (B_{ss}) when the magnet is expected to quench, the current in the cable at that time (I_c) and the current density (S_{quench}) in copper to carry that current. A lower current density in copper is expected to give a better stability. We have also given the current density in copper at 6.6 tesla ($S_{6.6T}$). When comparing the two cases in a table, $S_{6.6T}$ is a more appropriate parameter to consider than S_{quench}.

The design estimates of quench field etc. have been listed in the Table 7. They presume a degradation of 5% (J_c=2612.5), bath temperature of 4.35° kelvin and a copper to superconductor ratio of 1.8 in the outer layer and of 1.5 in the inner layer. The quench field of 7.273 tesla in the inner layer gives a field margin of 10.2% over the design operating field of 6.6 tesla. The quench field of 7.445 tesla in the outer layer gives a field margin of 12.8%.

Estimating the Effect of Random Errors

Due to various reasons the actual value of a parameter used in designing the coil may come out to be some what different than desired. In particular, we are interested in variations in the locations of the turns in the coil. This causes a change in the transfer function and field harmonics. In this section the effect of these errors in various cases are estimated using the procedure developed by P.A. Thompson[4]. The basic four fold symmetry in the dipole coil geometry is retained in this analysis. Though this is not a realistic assumption, it is useful in estimating the size of some random errors. In Table 9 these effects are listed for a nominal 0.05 mm variation in the given parameter. First we have given the effect of changing the radius of every turn in each current block by +0.05 mm. The counting of the blocks in the table is done by starting from the inner layer and from the midplane of each layer as shown in Fig. 5. Next we estimate the effect of changing the wedge size by +0.05 mm. Pole angle is held constant in this calculation by reducing the conductor thickness by an appropriate amount. The counting scheme

Table 9: The effect of 0.05 mm change in the given parameter on the transfer function and the field harmonics.

Parameter changed	TF T/kA	b_2' 10^{-4}	b_4' 10^{-4}	b_6' 10^{-4}
Block No. 1	0.31	-0.25	-0.10	-0.01
Block No. 2	-0.32	0.31	0.12	0.01
Block No. 3	-0.12	0.36	-0.02	-0.01
Block No. 4	-0.20	0.33	-0.08	0.01
Block No. 5	-0.11	-0.04	-0.01	0.00
Block No. 6	-0.78	0.22	0.03	0.00
RMS Blocks	0.38	0.27	0.07	0.01
Wedge No. 1	-1.56	-0.48	0.02	0.01
Wedge No. 2	0.83	0.59	0.05	-0.01
Wedge No. 3	2.32	0.71	-0.04	0.00
Wedge No. 4	-0.57	-0.11	0.00	0.00
RMS Wedges	1.48	0.52	0.03	0.01
Cable thickness inner	2.63	1.08	0.05	-0.01
Cable thickness outer	1.99	0.48	0.02	0.00
RMS Cable thickness	2.33	0.83	0.04	0.01
Pole angle inner	-4.01	-0.45	0.06	-0.01
Pole angle outer	-2.26	-0.42	0.00	0.00
RMS Pole angles	3.25	0.43	0.04	0.01

Table 10: Stored Energy and Inductance calculations at 6.5 kA.

	POISSON	PE2D
Stored Energy per unit length, kJ/m	105.0	105.3
Stored Energy for 15 m long Dipole, kJ	1575.6	1579.8
Inductance per unit length, mH/m	4.972	4.986
Inductance for 15 m long Dipole, mH	74.585	74.783

for the wedges is the same as it was for the current blocks. It is possible that during the molding, the thickness of the cable does not get reduced uniformly within a layer. To estimate this effect, a linear change in the cable thickness is assumed in going from the midplane to pole such that the middle turn is displaced azimuthally by 0.05 mm. The pole angle does not change during this perturbation. This effect is given for the inner and outer layers in the next two rows of this table. We also estimate the effect of increasing the pole angle by 0.05 mm in the inner and in the outer layer. We also compute the Root Mean Square (RMS) change for each group of these variations.

Stored Energy and Inductance Calculations

We have done stored energy calculations with the computer codes POISSON and PE2D at 6.5 kA (6.6 tesla). The results are given in Table 10. In this table we have given the stored energy and inductance for per unit length and as well as for a 15 m long dipole. The inductance has been computed using the relation

$$Stored\ Energy = \tfrac{1}{2} Inductance \times (Current)^2.$$

Lorentz Force Calculations

The value of Lorentz force on each turn is obtained from the components of the magnetic field (B_x, B_y) which are calculated using the program MDP. However, B_x and B_y are not uniform in a turn. We obtain the average values of these components from a grid of 10 × 2 across the width and thickness of the cable.

The variation in the magnitude of the radial and azimuthal components of the Lorentz force, namely F_r and F_θ, with the turn number is shown in Fig. 7. The turn numbers are counted from the midplane. The values of the components of the Lorentz force (F_x, F_y) and $(F_r,\ F_\theta)$ is given in Table 11.

The Lorentz force acts on the coil such that the azimuthal component compresses the coil on the midplane and the radial component expands it outward. Though the radial force on the turns in the outer layer is very small, the force on the turns in the inner layer must be transmitted through the outer layer to the structure of the magnet. In Fig. 8 we have shown the direction and magnitude of the total force in each block. The arrows represent the size and the magnitude of the force. Please note that the force in a block is a vector sum of the force acting on the individual turns of that block.

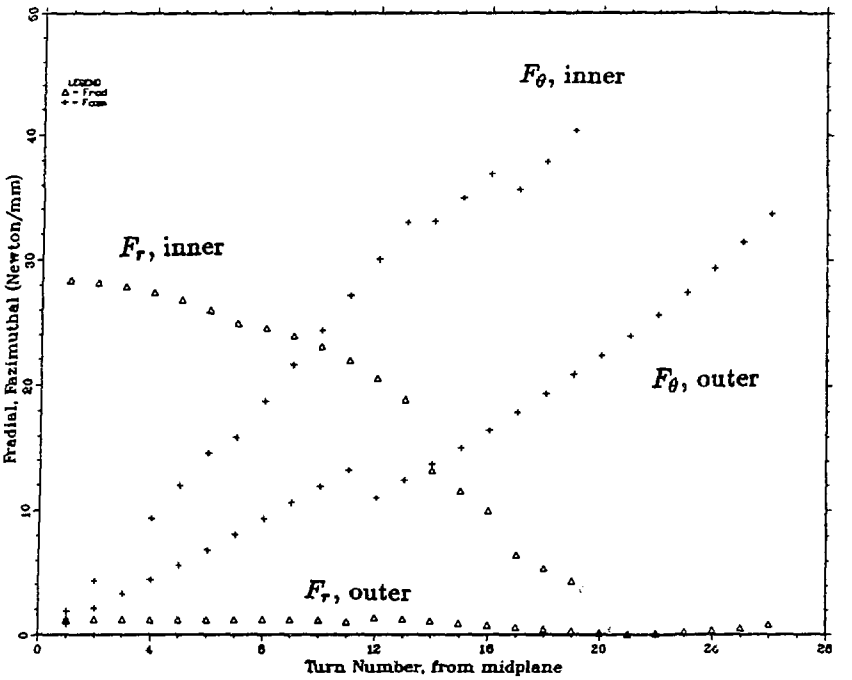

Figure 7: Magnitude of the Lorentz Force on each turn.

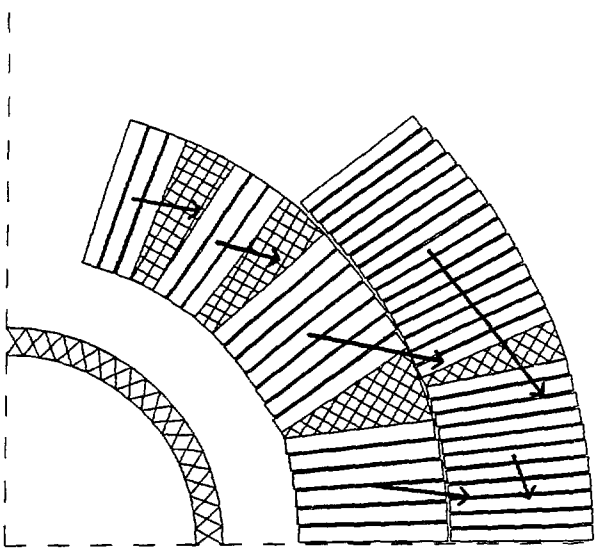

Figure 8: Lorentz Force on each block.

Table 11: Lorentz Force on each turn in SSC 50 mm dipole at 6500 ampere.

Turn No.	F_x N/mm	F_y N/mm	F_r N/mm	F_θ N/mm
Inner	layer			
1	28.42	-0.70	28.37	-1.82
2	28.48	-1.73	28.21	-4.31
3	28.60	-2.78	27.91	-6.82
4	28.76	-3.88	27.47	-9.36
5	28.97	-5.05	26.86	-11.96
6	29.21	-6.35	26.06	-14.65
7	29.49	-3.11	24.99	-15.96
8	30.67	-4.24	24.60	-18.80
9	31.81	-5.36	23.95	-21.60
10	32.96	-6.50	23.08	-24.41
11	34.13	-7.70	21.96	-27.24
12	35.33	-8.99	20.58	-30.09
13	36.61	-10.39	18.94	-33.01
14	34.42	-9.27	13.21	-33.11
15	35.55	-9.98	11.54	-35.08
16	36.90	-10.47	9.98	-37.04
17	35.57	-7.45	6.47	-35.77
18	37.69	-7.32	5.44	-38.01
19	40.08	-7.03	4.41	-40.45
Outer	layer			
1	1.20	-0.81	1.18	-0.84
2	1.28	-1.98	1.17	-2.04
3	1.43	-3.13	1.16	-3.24
4	1.66	-4.28	1.16	-4.44
5	1.97	-5.43	1.16	-5.65
6	2.35	-6.56	1.17	-6.87
7	2.81	-7.69	1.19	-8.10
8	3.34	-8.81	1.20	-9.35
9	3.94	-9.92	1.19	-10.61
10	4.56	-11.04	1.14	-11.89
11	5.20	-12.23	1.00	-13.25
12	5.56	-9.59	1.34	-11.01
13	6.34	-10.72	1.24	-12.39
14	7.13	-11.81	1.08	-13.76
15	7.99	-12.89	0.90	-15.13
16	8.92	-13.94	0.73	-16.54
17	9.95	-14.96	0.56	-17.96
18	11.08	-15.95	0.41	-19.42
19	12.31	-16.90	0.27	-20.91
20	13.64	-17.83	0.14	-22.45
21	15.09	-18.73	0.02	-24.05
22	16.66	-19.60	-0.08	-25.72
23	18.35	-20.46	-0.19	-27.49
24	20.18	-21.34	-0.32	-29.37
25	22.15	-22.27	-0.51	-31.41
26	24.34	-23.36	-0.80	-33.72

Summary of the Design

In this section we present the summary of this design. It includes various dimensions and the expected performance of this cross section. The summary is given in Table 12. Please note that the number of turns are the number of turns in each quadrant. The field margin in this cross section is limited by the inner layer. If the cable used in the inner layer has a copper to superconductor ratio of 1.3, the margin would be over 12%.

Table 12: Summary of SSC 50 mm Dipole Cross section

COIL	
Total No. of Turns ..	45
Number of Layers ...	2
Inner Layer	
No. of Turns	19
Strand Diameter, mm	0.808
Strands per turn	30
Coil i.d., mm	49.56
Coil o.d., mm	74.88
B_{peak}/B_o Ratio	1.048
Cu/Sc Ratio	1.5
Margin over 6.6 T ...	10.2%
Outer Layer	
No. of Turns	26
Strand Diameter, mm	0.648
Strands per turn	36
Coil o.d., mm	99.42
B_{peak}/B_o Ratio	0.869
Cu/Sc Ratio	1.8
Margin over 6.6 T ...	12.8%
IRON	
Inner Diameter, mm .	135.6
Outer Diameter, mm	330.2
Saturation Effects	
$\delta(TF)$, till 6.6 T	2.6%
δb_2, prime unit	0.3
δb_4, prime unit	0.03

References

1. R.C. Gupta, S.A. Kahn, G.H. Morgan, "DSX201/W6733 - Coil and Iron Design for SSC 50 mm Dipole Magnet with Wider Cable", SSC Technical Note No. 88 (SSCL-N-699), June 28,1990.

2. SSC 50 mm Dipole Task Force headed by R. Palmer.

3. SSC Conceptual Design Report, SSC-SR-2020, March 1986.

4. PAR2DOPT is an analytic coil design program which is presently maintained and developed by P. Thompson. This is a modified version of a program which was mostly written earlier by R. Fernow and later in part by G. Morgan.

DISCLAIMER

This report was prepared as an account of work sponsored by an agency of the United States Government. Neither the United States Government nor any agency thereof, nor any of their employees, makes any warranty, express or implied, or assumes any legal liability or responsibility for the accuracy, completeness, or usefulness of any information, apparatus, product, or process disclosed, or represents that its use would not infringe privately owned rights. Reference herein to any specific commercial product, process, or service by trade name, trademark, manufacturer, or otherwise does not necessarily constitute or imply its endorsement, recommendation, or favoring by the United States Government or any agency thereof. The views and opinions of authors expressed herein do not necessarily state or reflect those of the United States Government or any agency thereof.